High resolution rapid response observations of compact radio sources with the Ceduna Hobart Interferometer (CHI)

J. M. Blanchard[1,2], J. E. J. Lovell[1], R. Ojha[3,4], M. Kadler[5,6,7,8],
J. M. Dickey[1], and P. G. Edwards[2]

[1] School of Mathematics & Physics, Private Bag 37, University of Tasmania, Hobart TAS 7001, Australia
   e-mail: jayb@utas.edu.au
[2] Australia Telescope National Facility, CSIRO Astronomy and Space Science, PO Box 76, Epping, NSW 1710, Australia
[3] NASA, Goddard Space Flight Center, Greenbelt, MD 20771, USA
[4] Institute for Astrophysics & Computational Sciences (IACS), Dept. of Physics, The Catholic University of America,
   620 Michigan Ave., N.E., Washington, DC 20064, USA
[5] Institut für Theoretische Physik und Astrophysik, Universität Würzburg, Am Hubland, 97074 Würzburg, Germany
[6] Dr. Remeis Sternwarte & ECAP, Universität Erlangen-Nürnberg, Sternwartstrasse 7, 96049 Bamberg, Germany
[7] CRESST/NASA Goddard Space Flight Center, Greenbelt, MD 20771, USA
[8] Universities Space Research Association, 10211 Wincopin Circle, Suite 500 Columbia, MD 21044, USA

ABSTRACT

Context. Frequent, simultaneous observations across the electromagnetic spectrum are essential to the study of a range of astrophysical phenomena including active galactic nuclei. A key tool of such studies is the ability to observe an object when it flares i.e. exhibits a rapid and significant increase in its flux density.
Aims. We describe the specific observational procedures and the calibration techniques that have been developed and tested to create a single baseline radio interferometer that can rapidly observe a flaring object. This is the *only* facility that is dedicated to rapid high resolution radio observations of an object south of −30 degrees declination. An immediate application is to provide rapid contemporaneous radio coverage of AGN flaring at γ-ray frequencies detected by the *Fermi* Gamma-ray Space Telescope.
Methods. A single baseline interferometer, the Ceduna Hobart Interferometer (CHI), was formed with radio telescopes in Hobart, Tasmania and Ceduna, South Australia. A software correlator was set up at the University of Tasmania to correlate these data.
Results. Measurements of the flux densities of flaring objects can be made using our observing strategy within half an hour of a triggering event. These observations can be calibrated with amplitude errors better than 15%. Lower limits to the brightness temperatures of the sources can also be calculated using CHI.

Key words. instrumentation: interferometers – galaxies: jets – quasars: general – galaxies: active – galaxies: nuclei – gamma rays: galaxies

1. Introduction

The launch of the *Fermi* Gamma-ray Space Telescope (formerly GLAST; Atwood et al. 2009) on June 11th, 2008, has ushered in an era where it is possible to observe astronomical objects, including AGN, simultaneously across the entire electromagnetic spectrum. Such multiwavelength observations are essential to understand the behaviour of astronomical objects in general and AGN in particular. This motivated the TANAMI program (Tracking Active Galactic Nuclei with Austral Milliarcsecond Interferometry; Ojha et al. 2010) which provides radio monitoring of γ-ray loud sources (and a control sample) south of −30 degrees declination.

TANAMI observations are made at two radio frequencies using the telescopes of the Australian Long Baseline Array (LBA; e.g. Ojha et al. 2004) augmented by telescopes in South Africa, Chile, Antarctica and New Zealand. This array allows the imaging of the southern sky at milliarcsecond scale or better resolution on a regular basis (e.g., Müller et al. 2011). This observational technique, called Very Long Baseline Interferometry (VLBI), is essentially the only way to measure intrinsic parameters of the jets seen in AGN, as multi-epoch VLBI observations

provide the sole direct measurements of their relativistic motion (Cohen et al. 2007). They also play a crucial role in the identification of the nature and location of regions where γ-ray emission originates in AGN (Jorstad et al. 2001; Agudo et al. 2011). TANAMI VLBI observations are supported by radio monitoring programs at arc-second resolution using the Australia Telescope Compact Array (ATCA) and single-dish resolution using the Ceduna radio telescope (McCulloch et al. 2005). With its associated optical/UV and X-ray programs and its unique VLBI dual-frequency characteristics, TANAMI has become one of the major multiwavelength resources for the *Fermi* mission and the only one covering sources south of −30 degrees. TANAMI VLBI observations are constrained, however, by the availability of the LBA which only observes in approximately one week blocks every 2 ∼ 3 months. This makes it impossible to quickly observe a southern source that exhibits interesting behaviour such as rapid changes in flux density at one or more wavebands.

The Ceduna Hobart Interferometer (CHI) was developed to provide rapid, high resolution observations of sources in the southern sky. A fundamental characteristic of AGN is their variability at all wavelengths in which they are detected (Ulrich et al. 1997; Abdo et al. 2010). Thus a proper study of the physics of

AGN requires simultaneous multiwavelength observations, particularly when the flux density of an object changes significantly over a short period of time. Here we describe the specific observational procedures and calibration techniques that have been developed to create this uniquely useful single-baseline interferometer. It is important to note that, even though the development of CHI was motivated by the *Fermi* and TANAMI programs, it is by no means restricted to observations of γ-ray loud AGN but can be used for multiwavelength study of a range of compact sources e.g. optically flaring AGN, X-ray sources being studied by the INTEGRAL and *Swift* satellites, TeV sources detected by H.E.S.S., radio supernovae and some microquasars.

In this paper, we describe the CHI instrument in (Sect. 2) and describe our observing strategy (Sect. 3). We then explain our calibration procedures (Sect. 4) and present some results in Sect. 5. We end with a summary and description (Sect. 6) of further development planned for CHI. Throughout the paper we use the cosmology $H_0 = 73 \, \mathrm{km \, s^{-1} \, Mpc^{-1}}$, $\Omega_m = 0.27$, $\Omega_\Lambda = 0.73$ where the symbols have their traditional meanings.

2. CHI: The Ceduna Hobart Interferometer

The Ceduna Hobart Interferometer is a single baseline interferometer formed by a 26 m antenna located at Mount Pleasant, Hobart and a 30 m antenna located at Ceduna in South Australia. They are both re-purposed antennas that are now operated by the radio astronomy group at the University of Tasmania. CHI has a physical baseline length of 1704 km corresponding to a resolution of 6.6 milliarcsec at its current operating frequency of 6.7 GHz. The Hobart antenna is at latitude −42.8 degrees while the Ceduna antenna is at latitude −31.87. Thus CHI can, in principle, observe sources up to mid-northern latitudes and can easily observe the entire southern hemisphere.

The 30 m telescope at Ceduna is a former Telstra Satellite Earth Station, that was converted to astronomical use after its acquisition by the University of Tasmania in 1995. Ceduna uses a standard alt-azimuth mount, with a slew rate of 40 degrees per minute on each axis and an elevation limit of 10 degrees. It is a critical component of the Australian LBA, providing the major east-west baselines. However, Ceduna is primarily used for single dish programs monitoring γ-ray bright AGN in support of the TANAMI program as well as intra day variable (IDV; Wagner & Witzel 1995) AGN in support of the MASIV (Microarcsecond Scintillation-Induced Variability; Lovell et al. 2003, 2008) program. Ceduna is capable of observations at 2.2, 4.8, 6.7, 8.4, 12.2 and 22 GHz using room temperature receivers. Since the peak variability in amplitude of scintillating AGN is expected to be close to a frequency of 6.7 GHz, IDV observations are carried out in this band. As receiver changes at Ceduna are not automated, the standard observing frequency for CHI was selected to be 6.7 GHz, allowing for a rapid change between observing programs. Despite being uncooled, the 6.7 GHz receiver has a system equivalent flux density (SEFD) of roughly 820 Jy, equivalent to that at Hobart. This is mostly due to the larger collecting area of the 30 m dish, as well as the focus type. Hobart is a prime focus instrument with more spillover than the tertiary system at Ceduna.

The 26 m telescope at Mount Pleasant was opened on 13 May 1986 after having been moved from Orroral Valley in the Australian Capital Territory where it had been a NASA tracking station for about two decades. It also is a component of the Australian LBA and a vital geodetic antenna regularly participating in International VLBI Service (IVS; Schlüter & Behrend 2007) observations. Hobart uses a non traditional X-Y mount

Table 1. Brightness temperature sensitivity.

Redshift	Shape	Brightness temperature[a] K
0	Gaussian	1×10^9
0	Sphere	0.5×10^9
0	Disc	0.4×10^9
1	Gaussian	2.2×10^9
1	Sphere	1×10^9
1	Disc	0.8×10^9

Notes. [a] For a 1 jansky source.

slewing at 40 degrees per minute on both axes to an elevation limit of 7 degrees (apart from a 17 degree limit in the keyhole) and can observe at all major astronomical frequencies from 1.4 through 22 GHz. The 6.7 GHz receiver at Hobart is cooled to 20 K using helium cryogenics, giving a system equivalent flux density of approximately 820 Jy. The backend system at both telescopes produces two channels (right and left hand circular polarisation) of 32 MHz bandwidth. The baseline sensitivity of a 2 element interferometer is given by Eq. (1) (Thompson et al. 2001).

$$\Delta S_{ij} = \frac{1}{\eta_s} \sqrt{\frac{SEFD_i \times SEFD_j}{2 \Delta t \Delta \nu}} \qquad (1)$$

where η_s is the system efficiency (roughly 0.88 for 2 bit sampling), *SEFD* is the system equivalent flux density in Jy of each antenna, Δt is the integration time in seconds and $\Delta \nu$ is the bandwidth in MHz.

Thus, in just 60 s of integration time, CHI can reach a baseline sensitivity of about 15 mJy which is sufficient to observe all the sources in the TANAMI program. The coherence time at 6.7 GHz is approximately 4.6 min (calculated using the methods outlined in Briggs 1983 and checked against the given values in Walker 1995). This gives a maximum baseline sensitivity of approximately 7 mJy without phase referencing, more than enough to detect the above mentioned sources. Table 1 lists the brightness temperature sensitivity of CHI to a hypothetical 1 Jansky source for a range of parameters.

CHI data are recorded to disk at 256 Mbps at 2 bit sampling with the LBA Data Recorder system (Phillips et al. 2009) and the Ceduna disks are shipped to Hobart for correlation. The data are correlated using an installation of the DiFX software correlator (Deller et al. 2007). The correlator itself consists of a cluster of 6 PCs each containing dual quad-core Xeon processors and 3 GB of memory. The correlator can manage data rates of up to 512 Mbps on a single baseline, giving a 2 times real time correlation speed for a typical CHI observation. The biggest constraint on the speed of analysis of data from CHI however is the time taken for disks from Ceduna to be shipped to the correlator in Hobart. This means a typical turn around time of around 5 days for data to be fully reduced. Transfer over network is not possible due to the limited network capacity to Ceduna and the volume of data recorded.

3. Observing strategy for flaring AGN

Due to the peculiar calibration needs of a single baseline interferometer (see Sect. 4) and the desire to obtain good absolute amplitude calibration, we have developed a non-standard observing strategy. A typical CHI observation runs for twelve hours. Each

hour consists of a roughly 50 min long scan on the target source and a ten minute scan of PKS B193−638, the primary amplitude calibrator of the ATCA. PKS B1934−638 is observed as traditional amplitude calibration is not possible with a single baseline (see Sect. 4 for a discussion).

Observations are usually triggered following an increase in gamma-ray activity as found by the *Fermi*/LAT instrument. The flaring source is also added to the single dish monitoring program, providing a high cadence lightcurve at the observing frequency. If the source is observed to be flaring at radio frequencies multiple CHI observations are then undertaken to provide information on the state and evolution of the flare.

4. Calibration

Calibration of an interferometer with just two elements presents several interesting challenges. Since a minimum of 3 antennas are required for phase closure and 4 antennas for amplitude closure, it is not possible to use the standard VLBI tools of hybrid mapping (Readhead et al. 1980) or self-calibration (Pearson & Readhead 1984). Thus non-standard amplitude calibration must be performed on CHI data. Calibration requires two stages, a once off initial calibration and a calibration applied to each individual CHI observation.

4.1. Initial calibration

The need for amplitude calibration using a calibrator source is well met by PKS B1934−638, which has a flux density of 3.983 Jy at 6.7 GHz and does not vary significantly (Reynolds 1994). Unfortunately, at VLBI resolutions, PKS B1934−638 is not a point source and so a model is required in order to make amplitude calibration possible.

To create the model of PKS B1934−638, data from the V255 series of Australian LBA observations were used. The V255 project focuses on methanol maser studies at 6.7 GHz, making use of VLBI to measure accurate positions, distances and proper motions of these masers. PKS B1934−638 was observed in the V255 observations to act as a polarisation calibrator. Three epochs of V255 were used to make the model of PKS B1934−638 used for CHI. As part of the calibration the effect of elevation on the gain of the receiver must be corrected for. These gain-curves are not available for all LBA antennas at 6.7 GHz. Gain-curves from existing 8.4 GHz data were adjusted for the new frequency for telescopes that did not have 6.7 GHz curves available. For Ceduna the gain-curve was taken from McCulloch et al. (2005). For Hobart it is approximated as a first order polynomial and this may introduce a small elevation effect into CHI data (see Fig. 3).

Finally the absolute flux scale of the PKS B1934−638 model at 6.7 GHz was set using simultaneous ATCA and LBA data of several point sources (0506−612, 0808+019, 1022−665 and 1420−679). This was not possible to achieve using the PKS B1934−638 data itself as PKS B1934−638 is resolved on VLBI baselines. For a point source however the VLBI and ATCA fluxes should be the same and so the difference in VLBI and ATCA flux density was calculated for each of the point sources mentioned above, giving an average correction factor of 1.45 ± 0.2 used to scale the model of PKS B1934−638. This gave the final clean component model as seen in Figs. 1 and 2. The error in this correction factor (of order 15 percent) is by far the dominant form of error in flux density measurements made using CHI and is thus used as an estimate of the total error in such measurements.
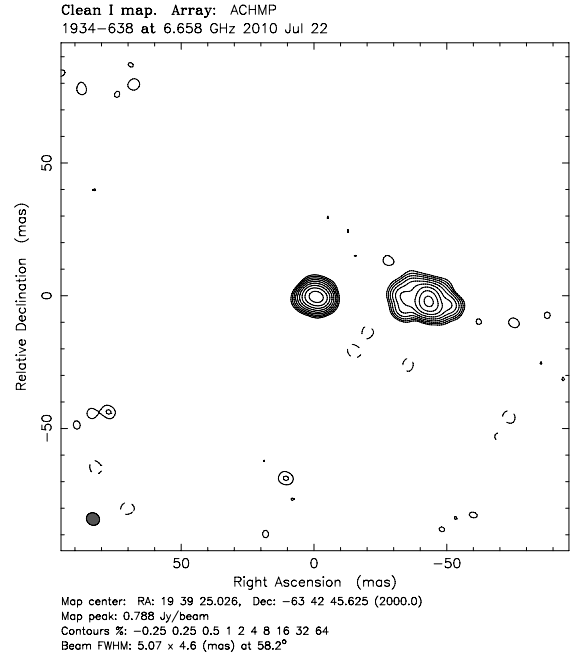
Fig. 1. The brightness distribution of PKS B1934−638 derived from the model created using AIPS and Difmap.
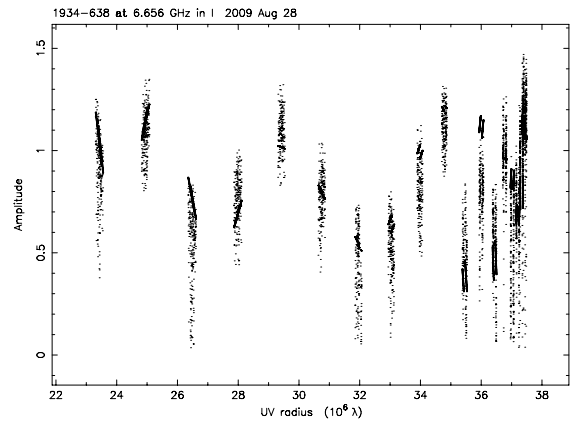

Fig. 2. Calibrated PKS B1934−638 amplitude vs. (u, v) distance plot with the overlaid model.

4.2. CHI calibration

As described in Sect. 3, PKS B1934−638 is observed in each CHI observation to perform additional amplitude calibration, as required by the single baseline. The CHI data (including both the target source(s) and PKS B1934−638) are initially calibrated in AIPS (Astronomical Image Processing System; Greisen 1998) in the standard manner. Fringe-fitting is carried out to correct for residual delay and rate errors. This is followed by amplitude calibration using the known gain-curves and system temperature measurements made at each antenna over the course of the experiment.

The AIPS calibrated PKS B1934−638 data are loaded into the Caltech difference mapping program "Difmap" (Shepherd et al. 1995) and the model created as described in Sect. 4.1 is then overlaid on an amplitude vs. (u, v) distance plot. A simple script is then used to manipulate the model to fit both the amplitude vs. (u, v) distance plot (see Fig. 2) and an amplitude vs. time plot, giving a correction factor.
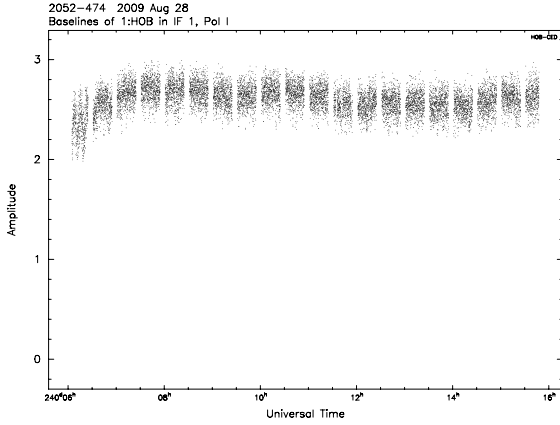
Fig. 3. Amplitude vs. time plot for the calibrated 2052−474 observation. Note the downturn in amplitude at the beginning of the experiment. This corresponds to low elevation of the source and is thus likely a residual elevation effect. This is perhaps due to the simple nature of the gain-elevation curve for the Hobart Antenna.

This correction factor is then used to scale the visibilities of the baseline producing the final calibrated source observation.

5. Results

We present a typical CHI observation. PKS 2052−474 is a blazar at a redshift of 1.489. It is established to be a variable gamma-ray source. Abdo et al. (2010) show a light curve with two flaring events, occurring around February and June 2009 respectively. Previous VLBI observations have found the source to be strongly core dominated on the milli-arcsecond scale (Ojha et al. 2010, 2004; Piner et al. 2007). On the kilo-parsec scale, ATCA imaging shows some extended structure (Marshall et al. 2005; Burgess & Hunstead 2006) extending over 4 arcsec. The observation presented here was made in support of a *Fermi*/LAT multiwavelength campaign on this object in 2009 (Chang et al. 2010) following the flaring seen in the gamma-ray.

Calibration was performed as explained in Sect. 4, resulting in the amplitude vs. time plot seen in Fig. 3 and the amplitude vs. (u, v) distance plot seen in Fig. 6. This is consistent with a point source with a flux density of 2.6 Jy. Figure 5 shows single dish data from the Ceduna monitoring program, as well as ATCA data from the C1730 gamma-ray sources monitoring program, around the time of the CHI observation. The flux density obtained from the CHI observations is consistent with that of the single dish data (as expected for an unresolved source) giving us confidence in the amplitude calibration technique employed by CHI. The (u, v) coverage of a typical CHI observation is shown in Fig. 4. Applying the radiometer equation (Eq. (1)) to this 7 h observation of PKS 2052−474 gives an expected noise of 0.73 mJy rms, agreeing well with the observed noise in the visibilities of 0.75 mJy rms.

A constraint on the angular size of the source can be calculated by applying a Gaussian model to the visibilities. For this example observation of 2052−474 a model with an angular size of 0.8 mas is chosen, as the visibilities are well encompassed by the model (see Fig. 6). Note that we are not trying to fit to the data directly, rather we are choosing a Gaussian which lies below the majority of the visibilities, thus providing an upper limit to the angular size.
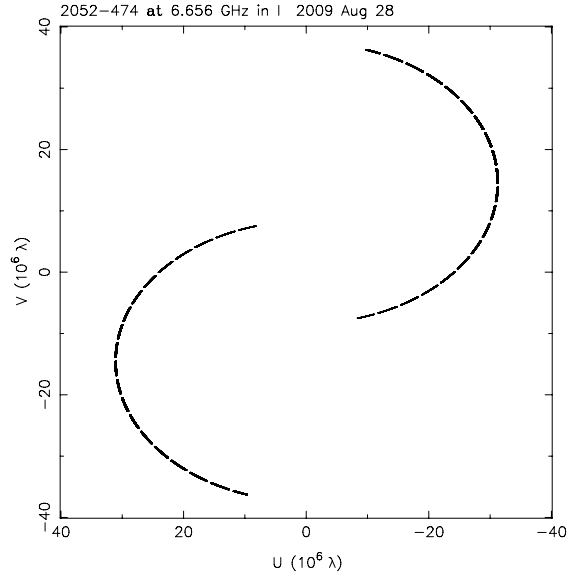
Fig. 4. The (u, v) coverage obtained from a 12 h CHI observation of 2052-474. This is typical of a CHI experiment.
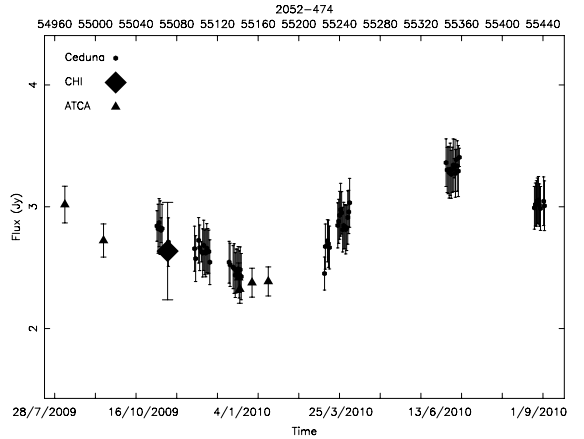
Fig. 5. Single dish and ATCA monitoring data of PKS 2052−474 overlaid with the CHI observation (the large filled diamond). The Ceduna data are the circles and the ATCA data the triangles. The VLBI data is consistent with both the single dish and the ATCA monitoring flux density. Note that the ATCA data are interpolated between simultaneous 5.5 and 9 GHz data to match the 6.7 GHz Ceduna single dish data.

The brightness temperature of a source is given by

$$T_b = \frac{2 \ln 2}{\pi k} \frac{S_\nu \lambda^2 (1+z)}{\theta_{\mathrm{maj}} \theta_{\mathrm{min}}} \qquad (2)$$

where k is Boltzmann's constant, S_ν is the flux density of the source, z is its redshift and θ the angular size (see for example Kovalev et al. 2005).

Using the upper limit to the angular size of the source and Eq. (2), a lower limit of 2×10^{11} K for the brightness temperature is calculated. This is well below the inverse compton limit.

6. Summary and future developments

The CHI interferometer is the only facility capable of rapid, high resolution observations of compact radio sources south of about −30 degrees declination. The peculiar calibration challenges of such a single baseline interferometer have been met and initial
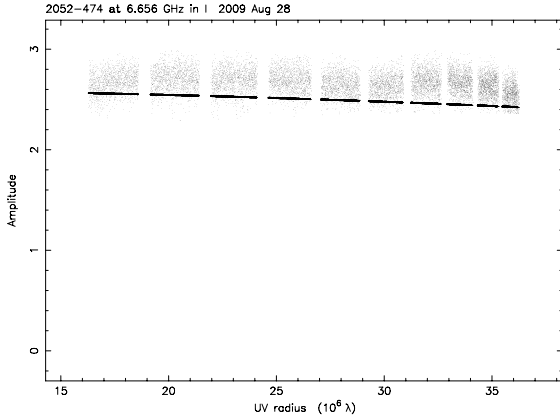
Fig. 6. Amplitude vs. (u, v) distance plot of the calibrated 2052–474 CHI data. A model with major axis of 0.8 mas and an axial ratio of 1 well constrains the visibilities, giving an upper limit on the angular size of the source. Note the choice of model is not a fit to the data but rather lies below the majority of points to give an upper limit to the angular size.

results are presented. Currently CHI is a critical component in the multiwavelength study of AGN in the age of *Fermi*. However, its role is set to be broader as it is capable of observing any type of compact radio source in the southern sky with high sensitivity.

There are three developments under active consideration for CHI. First, observation at multiple radio frequencies would provide radio spectral index measurements which are very useful inputs to models of the emission from AGN. Both Hobart and Ceduna can observe at the standard centimeter wavelength radio bands. We will develop the calibration at additional frequencies of 2.3, 8.4 and 22 GHz, in order to make CHI capable of spectral index measurements.

Second, while CHI observations can be initiated almost instantly, the remote nature of the Ceduna observing site makes the shipping of data to the correlator in Hobart the biggest bottleneck to rapid analysis. The possibility of taking preliminary measurements using a "sniffing" strategy is being explored. This would involve taking short (about one second) slices of the twelve hours of data and transferring them back via network, thus decreasing the transfer time without sacrificing (u, v) coverage too much. This would allow a quick analysis showing the flaring state of a target (for example) where such information is needed to trigger observations at other wavelengths.

Finally, we are investigating the possibility of including the new 12 m antenna at Warkworth, New Zealand (Gulyaev et al. 2011) in the CHI array. This would increase the maximum baseline to 3724 kilometers boosting the resolution 2.5 times

at an observing frequency of 8.4 GHz, as well as providing phase closure.

References

Abdo, A. A., Ackermann, M., Ajello, M., et al. 2010, ApJ, 722, 520
Agudo, I., Jorstad, S. G., Marscher, A. P., et al. 2011, ApJ, 726, L13
Atwood, W. B., Abdo, A. A., Ackermann, M., et al. 2009, ApJ, 697, 1071
Briggs, F. H. 1983, AJ, 88, 239
Burgess, A. M., & Hunstead, R. W. 2006, AJ, 131, 114
Chang, C. S., Ros, E., Kadler, M., et al. 2010 [arXiv:1001.1563]
Cohen, M. H., Lister, M. L., Homan, D. C., et al. 2007, ApJ, 658, 232
Deller, A. T., Tingay, S. J., Bailes, M., & West, C. 2007, PASP, 119, 318
Greisen, E. W. 1998, in Astronomical Data Analysis Software and Systems VII, ed. R. Albrecht, R. N. Hook, & H. A. Bushouse, ASP Conf. Ser., 145, 204
Gulyaev, S., Natusch, T., Weston, S., et al. 2011 [arXiv:1103.2830]
Jorstad, S. G., Marscher, A. P., Mattox, J. R., et al. 2001, ApJ, 556, 738
Kovalev, Y. Y., Kellermann, K. I., Lister, M. L., et al. 2005, AJ, 130, 2473
Lovell, J. E. J., Jauncey, D. L., Bignall, H. E., et al. 2003, AJ, 126, 1699
Lovell, J. E. J., Rickett, B. J., Macquart, J. P., et al. 2008, ApJ, 689, 108
Marshall, H. L., Schwartz, D. A., Lovell, J. E. J., et al. 2005, ApJS, 156, 13
McCulloch, P. M., Ellingsen, S. P., Jauncey, D. L., et al. 2005, AJ, 129, 2034
Müller, C., Kadler, M., Ojha, R., et al. 2011, A&A, 530, L11
Ojha, R., Fey, A. L., Johnston, K. J., et al. 2004, AJ, 127, 3609
Ojha, R., Kadler, M., Böck, M., et al. 2010, A&A, 519, A45
Pearson, T. J., & Readhead, A. C. S. 1984, ARA&A, 22, 97
Phillips, C., Tzioumis, T., Tingay, S., et al. 2009, in Proc. 8th Int. e-VLBI Workshop, 99
Piner, B. G., Mahmud, M., Fey, A. L., & Gospodinova, K. 2007, AJ, 133, 2357
Readhead, A. C. S., Walker, R. C., Pearson, T. J., & Cohen, M. H. 1980, Nature, 285, 137
Reynolds, J. E. 1994, A revised flux scale for the AT Compact Array, ATNF Memo AT/39.3/040
Schlüter, W., & Behrend, D. 2007, J. Geodesy, 81, 379
Shepherd, M. C., Pearson, T. J., & Taylor, G. B. 1995, in BAAS 27, ed. B. J. Butler & D. O. Muhleman, 903
Thompson, A., Moran, J., & Swenson, G. 2001, Interferometry and synthesis in radio astronomy (Wiley)
Ulrich, M. H., Maraschi, L., & Urry, C. M. 1997, ARA&A, 35, 445
Wagner, S. J., & Witzel, A. 1995, ARA&A, 33, 163
Walker, R. C. 1995, in Very Long Baseline Interferometry and the VLBA, ed. J. A. Zensus, P. J. Diamond & P. J. Napier, ASP Conf. Ser., 82, 133